Scandinavian Journal of Gastroenterology. 2015; 50: 429–438

informa
healthcare

ORIGINAL ARTICLE

Simultaneous liver iron and fat measures by magnetic resonance imaging in patients with hyperferritinemia

STEFANIA GALIMBERTI*[1], PAOLA TROMBINI*[2], DAVIDE PAOLO BERNASCONI[1], IRENE REDAELLI[3], SARA PELUCCHI[4], GIORGIO BOVO[5], FILIBERTO DI GENNARO[6], NICOLA ZUCCHINI[5], NICOLETTA PARUCCINI[3] & ALBERTO PIPERNO[4,7]

[1]*Department of Health Sciences, Centre of Biostatistics for Clinical Epidemiology, University of Milano-Bicocca, Monza, Italy,* [2]*Internal Medicine Unit, ICP Sesto S.Giovanni Hospital, Milan, Italy,* [3]*Medical Physics Unit, S.Gerardo Hospital, Monza, Italy,* [4]*Department of Health Sciences, University of Milano-Bicocca, Monza, Italy,* [5]*Clinical Pathology Unit, S.Gerardo Hospital, Monza, Italy,* [6]*Clinical Radiology Unit, S.Gerardo Hospital, Monza, Italy, and* [7]*Centre for Hemochromatosis and Iron Metabolism Disorders, S.Gerardo Hospital, Monza, Italy*

Abstract

Objective. Hyperferritinemia is frequent in chronic liver diseases of any cause, but the extent to which ferritin truly reflects iron stores is variable. In these patients, both liver iron and fat are found in variable amount and association. Liver biopsy is often required to quantify liver fat and iron, but sampling variability and invasiveness limit its use. We aimed to assess single breath-hold multiecho magnetic resonance imaging (MRI) for the simultaneous lipid and iron quantification in patients with hyperferritinemia. ***Material and methods.*** We compared MRI results for both iron and fat with their respective gold standards – liver iron concentration and computer-assisted image analysis for steatosis on biopsy. We prospectively studied 67 patients with hyperferritinemia and other 10 consecutive patients were used for validation. We estimated two linear calibration equations for the prediction of iron and fat based on MRI. The agreement between MRI and biopsy was evaluated. ***Results.*** MRI showed good performances in both the training and validation samples. MRI information was almost completely in line with that obtained from liver biopsy. ***Conclusion.*** Single breath-hold multiecho MRI is an accurate method to obtain a valuable measure of both liver iron and steatosis in patients with hyperferritinemia.

Key Words: *ferritin, iron, liver, magnetic resonance imaging, steatosis*

Introduction

Hyperferritinemia is frequently observed in chronic liver diseases such as chronic viral hepatitis, alcoholic liver diseases, nonalcoholic fatty liver disease (NAFLD), and nonalcoholic steatohepatitis, but the extent to which ferritin reflects iron stores in these conditions is variable [1]. Nevertheless, mild-to-moderate hepatic iron overload is commonly observed in many chronic liver disorders [2]. Moreover, an intriguing association between hyperferritinemia, iron overload, insulin resistance, alterations of the metabolic syndrome (MetS), and NAFLD has been described and later designed as dysmetabolic iron overload syndrome (DIOS) [3–6]. DIOS is a common condition, occurring in 15–20% of patients with MetS [7,8] and in about one-third of subjects with NAFLD [9]. It represents the most severe counterpart of the so-called dysmetabolic hyperferritinemia [4] that is by far the commonest cause of consultation for hyperferritinemia in clinical practice [10]. The clinical significance of such secondary iron loading is controversial, but some studies suggest that it might contribute to hepatic fibrosis [4] together

Correspondence: Alberto Piperno, Clinical Medicine, S. Gerardo Hospital, Via Pergolesi n. 33, 20900 Monza, Italy. Tel: +39 039 233 9710 9555. Fax: +39 039 2333349. E-mail: alberto.piperno@unimib.it
*Stefania Galimberti and Paola Trombini have equally contributed to the paper.

(Received 25 March 2014; accepted 24 June 2014)

ISSN 0036-5521 print/ISSN 1502-7708 online
DOI: 10.3109/00365521.2014.940380

with NAFLD that is a growing cause of cirrhosis and hepatocellular carcinoma [11]. Thus, both intrahepatic fat fraction (FF) and liver iron concentration (LIC) denote important parameters to be evaluated in the diagnostic and therapeutic settings in patients with hyperferritinemia.

Liver biopsy is currently the gold standard to assess LIC and intrahepatic lipid content [12,13], although sampling variability and invasiveness limit its use. In addition, the standard estimation of the percentage of fat-containing hepatocytes cannot be a precise measure of steatosis [14]. Area of steatosis (AOS), computed by digital image analysis, can be more representative of triglyceride content but requires specific software and skilled personnel [15,16]. Recent evidences indicate that magnetic resonance imaging (MRI) accurately quantifies hepatic iron content in thalassemia patients [17,18], but data on the accuracy of MRI in other iron overload diseases are rather limited. MRI is also effective for steatosis assessment [13,19], but the presence of iron is a potential pitfall in the quantification of liver fat [20,21]. Single breath-hold multiecho MRI sequences have the potential to enable the simultaneous fat and iron quantification in a very short time (about 20 s) [22].

Aim of the study was to investigate single breath-hold multiecho MRI sequences (at 1.5T) for the simultaneous hepatic iron and lipid quantification in patients with hyperferritinemia by comparing MRI results with their respective gold standards, LIC and AOS measured on liver biopsy specimens.

Materials and methods

Patients

This was a prospective study that included 67 patients with increased serum ferritin levels who underwent abdominal MRI examination and liver biopsy for diagnostic purposes from June 2008 to May 2010.

Other 10 consecutive patients with hyperferritinemia (10 men with a median age of 51.4 years) who performed both MRI and liver biopsy between January 2011 and January 2012 were used as validation sample. Additional patients' details are in Supplementary Materials and Methods.

The study was done at the Center for Disorders of Iron Metabolism at the S.Gerardo Hospital in Monza. Each patient gave written informed consent to the study protocol that conforms to the Declaration of Helsinki and was approved by the institution's ethics committee.

Magnetic resonance imaging

Magnetic resonance examinations were performed on a 1.5T whole-body scanner (Achieva 1.5T SE; Philips Medical Systems, Best, the Netherlands) close to liver biopsy (median = -20 days from biopsy). No therapies were started during this period. A 20 echo Gradient-Echo sequence was employed (TE = 1.05 ms, ΔTE = 1.05 ms, TR = 150 ms, flip angle 35, FOV: RL = 400 mm, AP = 300 mm, FH = 10 mm voxel size: RL = 3.12 mm, AP = 3.12 mm slice thickness = 10 mm, slices number = 1, acquisition matrix = 128*96) and was performed in breath-hold, resulting in a total acquisition time of around 20 s with Sense-body coil. Images were analyzed using Image J (National Institute of Health, USA) and Datafit 7.1 (Oakdale, CA, USA) software (see Supplementary Materials and Methods, for details). The magnitude of the signal intensity (S) is expressed by a bi-exponential equation: $|S| = |S_w e^{-t/T2^{\star}w} + S_f e^{-t/T2^{\star}f+i\Delta\omega\ t}|$, where S_w and S_f are the signal of water and fat, $T2^{\star}_w$ and $T2^{\star}_f$ are their relaxation time, t is the time after radio frequency excitation, and $\Delta\omega$ = 3.4 ppm is the difference in Larmor frequency between fat and water.

Fat fraction (FF), that is, the percentage of S_f on the total signal, was used for expressing the hepatic lipid content: $FF = 100[S_f/(S_w+S_f)]$ [22], whereas the relaxation rate $R2^{\star} = 1/T2^{\star}$, that is directly proportional to iron amount, was used for LIC.

Liver histopathology

Immediately after the procedure, a 2 cm piece of biopsy specimen (about 0.8 mm diameter) was fixed in 10% formalin (pH 7.4) and sent to the Pathology Unit, and a piece of at least 1 cm, when available, was collected for LIC measurement. Standard stains were used for routine histology and Perls' stain was used for iron grading. Specimens were reviewed by the same pathologist (GB). Liver fibrosis was graded according to Ishak et al. [23].

Quantification of liver iron. In 56 patients, liver biopsy specimens were adequate for LIC (LIC_{biopsy}) measurement, according to Barry and Sherlock [24]. LIC_{biopsy} was measured by atomic absorption spectrophotometry and expressed in micromole per gram dry weight. Based on LIC_{biopsy}, we classified iron overload in four categories (absent: ≤30, mild: >30 and ≤100, moderate: >100 and ≤200, and severe: >200 μmol/g), as previously reported [25]. Iron overload was also assessed by total iron score (TIS) as described by Deugnier et al. [26].

Quantification of liver steatosis. Steatosis was routinely evaluated by visual estimation of the percentage of fatty hepatocytes, according to Kleiner et al. [27]. For MRI comparison, computer-assisted morphometric assessment of area of steatosis (AOS_{biopsy}) was done by another pathologist (NZ) unaware of standard visual estimation. Image analysis was performed with ImageJ 1.42q software (National Institute of Health, USA, http://rsbweb.nih.gov/ij/) on 10× consecutive but not overlapping pictures, covering the entire liver specimen [16]. Hepatic steatosis was then classified into four categories (absent: ≤2, mild: >2 and ≤6, moderate: >6 and ≤15, and severe: >15%) based on the results described by Turlin et al. [16] and sustained by our data (see Supplementary Figure 1). Further details are in Supplementary Materials and Methods.

Statistical analysis

Mean and standard deviation or median and I–III quartiles were properly used for descriptive purposes. The selection of the optimal cut-off value of the MRI parameters that discriminated patients with low (normal-to-mild categories) or high (moderate-to-severe categories) iron and fat in the liver was based on the Youden Index. Calibration equations of MRI parameters for the prediction of iron and fat concentrations were obtained by linear regression on biopsy measures. Natural logarithm transformation was considered to improve calibration.

To investigate the agreement between MRI and biopsy in quantifying both hepatic iron and fat, the method of Bland and Altman was used and the 95% limits of agreement were calculated. The assumptions underlying this analysis were checked both graphically and by a regression approach [28]. The Cohen's weighted κ was also calculated to measure the agreement between biopsy and calibrated MRI measures on classification in the four ordered categories.

All the analyses were performed with SAS 9.3 (SAS Institute, Cary, NC, USA) and R 2.15.3.

Results

The main patients' characteristics are reported in Table I. The individual levels of steatosis and iron concentration are shown in Figure 1. The 11 patients in which LIC was not measured due to insufficient biopsy specimen did not represent a selected sample as their measures covered the full range of steatosis (AOS_{biopsy}: 0–25%) and iron overload (TIS: 12–36), respectively.

Table I. Characteristics of the 67 patients with hyperferritinemia who underwent MRI and liver biopsy.

Parameter	Results[a]
Age at liver biopsy (years)	50.5 (45.2–60)
Males	59 (88)
Fibrosis (grade)	
0–1	4 (6)
2–4	50 (75)
5–6	13 (19)
Hepatic iron	
Total iron score	15 (12–25)
Liver iron concentration[b] (μmol/g)	44.6 (26.4–81.6)
Hepatic fat	
Grading of fatty hepatocytes (%)	70.0 (25.0–90.0)
Area of steatosis (%)	9.5 (3.2–17.1)

[a]Results are reported as *n* (%) or median (I–III quartile).
[b]LIC_{biopsy} was missing in 11 subjects.
Abbreviation: LIC = Liver iron concentration.

Quantification of liver iron

The 56 available LIC_{biopsy} ranged from 9.9 to 481.6 μmol/g, with a median of 44.6 μmol/g (I–III quartiles = 26.4–81.6 μmol/g), whereas the R2⋆ measures obtained by MRI varied from 34.8 and 1140.7 sec^{-1}, with a median of 85.7 sec^{-1} (I–III quartiles = 61.1–154.2 sec^{-1}). The relationship between LIC_{biopsy} and R2⋆ is shown in Figure 2A. The R2⋆ cut-off value of 147.1 sec^{-1} discriminated patients with LIC ≤100 or >100 μmol/g with a 100% sensitivity (95% CI = 75.8–100%) and a 93.2% specificity (95% CI = 81.8–97.7%).

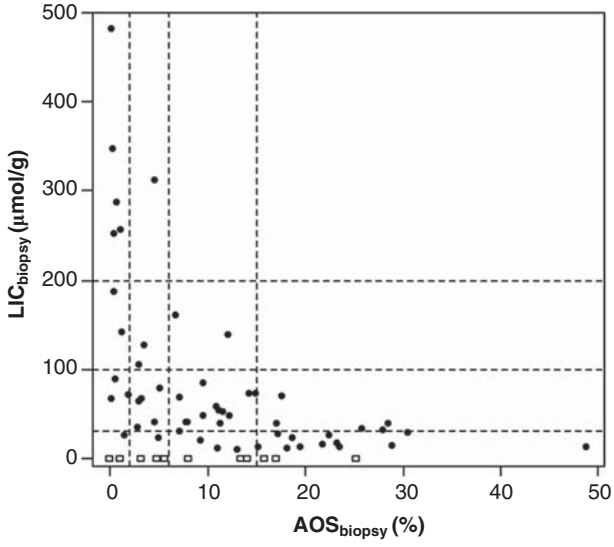

Figure 1. Hepatic steatosis (AOS) and iron (LIC) by histology in 56 patients are shown. The 11 patients with LIC missing are shown only in the AOS dimension with squares. Dashed lines represent the thresholds of the four categories of classification.
Abbreviations: AOS = Area of steatosis; LIC = Liver iron concentration.

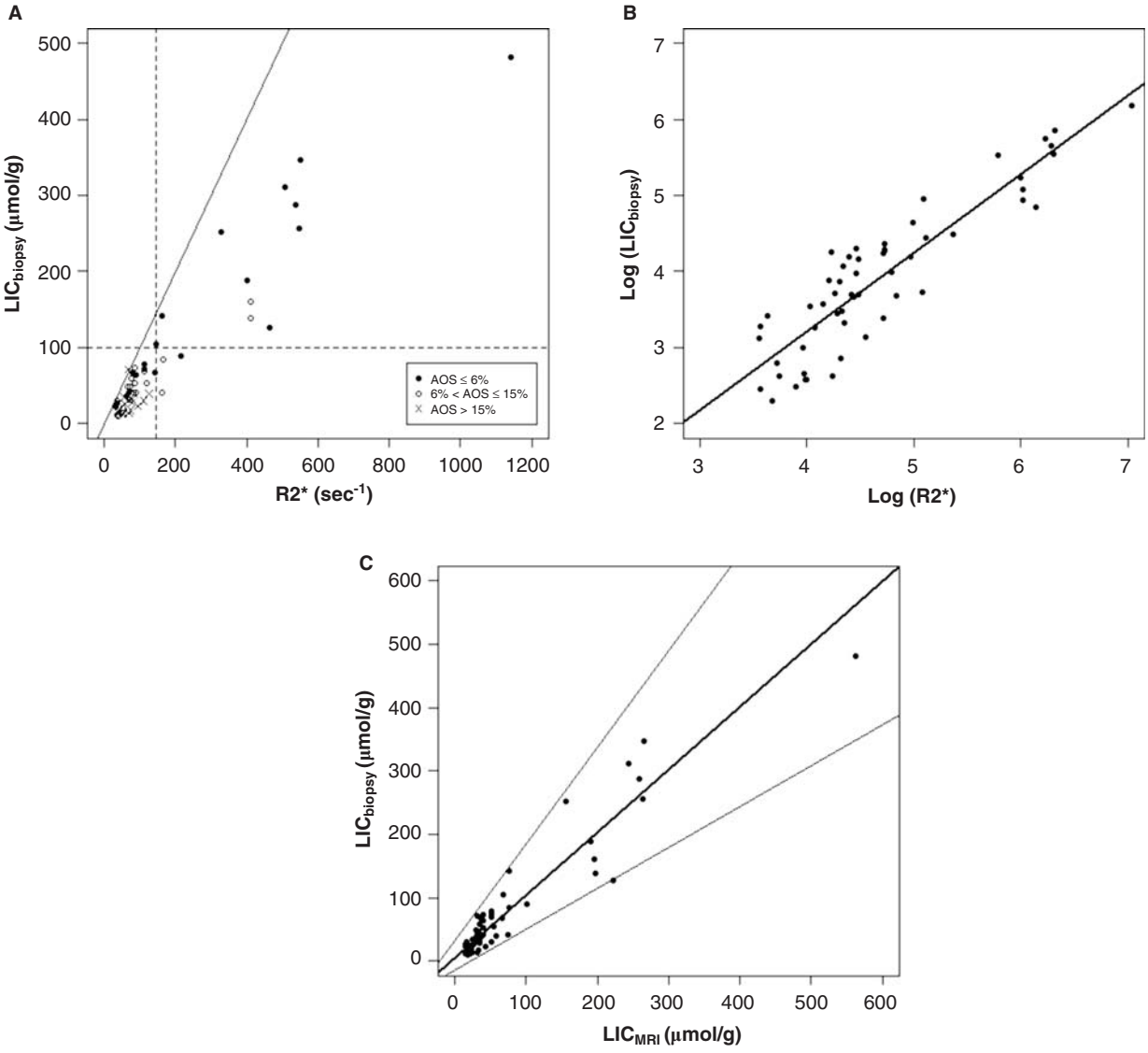

Figure 2. Quantification of hepatic iron by LIC through R2* is shown. (A) R2* versus LIC_{biopsy}. The 45° line of perfect agreement (continuous) and the cut-off lines for iron overload (dashed) are shown. (B) R2*-LIC_{biopsy} calibration line on natural logarithmic scale and (C) agreement between LIC_{biopsy} and LIC_{MRI} are shown. The solid line that represents the bias in using LIC_{MRI} to predict LIC_{biopsy} is superimposed to the 45° line of perfect agreement, whereas the two thin lines represent the 95% limits of agreement.
Abbreviations: AOS = Area of steatosis; LIC = Liver iron concentration.

In order to obtain a prediction of LIC based on R2* values (LIC_{MRI}), a linear calibration was performed on the logarithm of both LIC_{biopsy} and R2*, as illustrated in Figure 2B. The fitted model produced the following conversion formula: $\log(LIC_{MRI}) = -0.92 + 1.03\log(R2^*)$ ($R^2 = 0.81$), or equivalently, on the original scale of LIC: $LIC_{MRI} = 0.40R2^{*1.03}$. When the predicted values were compared to those obtained from biopsy, the mean difference between LIC_{biopsy} and LIC_{MRI} was uniformly close to zero (2.8 µmol/g) over the whole range of LIC measurements ($p = 0.514$), whereas their variation increased with the increasing of LIC values ($p < 0.0001$), as shown by the diverging limits of agreement in Figure 2C. When we assessed the agreement between the LIC_{biopsy} and LIC_{MRI} classification in four categories (absent, mild, moderate, and severe) (Table IIa), we had 48 correctly classified patients out of 56 (85.7%), with a weighted Cohen κ-index of 0.84 (95% CI = 0.74–0.95%). Discrepancies were mostly borderline misclassifications between absent and mild categories. In two patients, misclassifications were in the moderate-marked classes: one had a LIC_{biopsy} = 127 µmol/g, but a LIC_{MRI} = 223 µmol/g and 6.5 g of iron removed by phlebotomy and the other patient had a LIC_{biopsy} = 252.3 µmol/g and a LIC_{MRI} = 155.1 µmol/g, with

Table II. Agreement between observed and predicted values of hepatic iron (**a**)–(**b**) and fat (**c**) by MRI.

(a)

	LIC_{MRI}				
LIC_{biopsy}	Absent	Mild	Moderate	Severe	Total
Absent	14	3	0	0	17
Mild	2	26	0	0	28
Moderate	0	1	3	1	5
Severe	0	0	1	5	6
Total	16	30	4	6	56[a]

(b)

	$LIC_{MRI-AOS}$				
LIC_{biopsy}	Absent	Mild	Moderate	Severe	Total
Absent	17	0	0	0	17
Mild	4	23	1	0	28
Moderate	0	1	2	2	5
Severe	0	0	1	5	6
Total	21	24	4	7	56[a]

(**c**)

	AOS_{MRI}				
AOS_{biopsy}	Absent	Mild	Moderate	Severe	Total
Absent	4	1	0	0	5
Mild	1	9	1	0	11
Moderate	0	0	17	3	20
Severe	0	0	3	17	20
Total	5	8	22	21	56[b]

[a]LIC_{biopsy} was missing in 11 subjects.
[b]AOS_{MRI} was not available in 11 subjects because fat fraction was not obtained from the bi-exponential model due to the presence of too much iron.
Abbreviations: AOS = Area of steatosis; LIC = Liver iron concentration.
Gray cells indicate correct classification by MRI parameters.

4.2 g of iron removed. Thus, LIC_{MRI} appeared to be more reliable than LIC_{biopsy} as indicator of the amount of body iron in both patients.

Since the amount of iron was significantly related to the presence of steatosis, but not to fibrosis and liver sample weight (data not shown), a calibration regression model was considered to improve the goodness of fit (R^2 = 0.88). We obtained three conversion equations for the groups of patients with absent-to-mild (the latter categories were grouped because of very similar behavior), moderate, and severe levels of steatosis: $\log(LIC_{MRI-AOS}) = 0.12 + 0.87\log(R2^{\star})$, $\log(LIC_{MRI-AOS}) = -0.14 + 0.87\log(R2^{\star})$ and $\log(LIC_{MRI-AOS}) = -0.56 + 0.87\log(R2^{\star})$, respectively (Figure 3A). When considering steatosis in the calibration, the performance in terms of agreement between the measures of LIC_{biopsy} and LIC_{MRI} improved in precision, still retaining unbiased results (Figure 3B). However, the rate of correct classification in four categories (84%) and the weighted Cohen index (κ = 0.83, 95% CI = 0.74–0.93%) did not substantially change (Table IIb).

Quantification of liver steatosis

AOS_{biopsy} was available in all 67 patients with a median of 9.5% (I–III quartiles = 3.2–17.1%) and a range between 0.1% and 48.7%. The latter value, belonging to a patient with 99% fatty hepatocytes due to high dosage of corticosteroid therapy, was excluded from the analyses. The relation between AOS and percentage of hepatocytes containing fat is reported in Supplementary Figure 1.

MRI fat could not be quantified in 11 patients because the bi-exponential model was not appropriate due to the presence of too much iron. Interestingly, in these subjects values at biopsy were very low for both AOS_{biopsy} (median = 0.9%, I–III quartiles = 0.4–5.1%) and standard grading of steatosis (median = 3%, I–III quartiles = 3–12.5%). In addition, medians

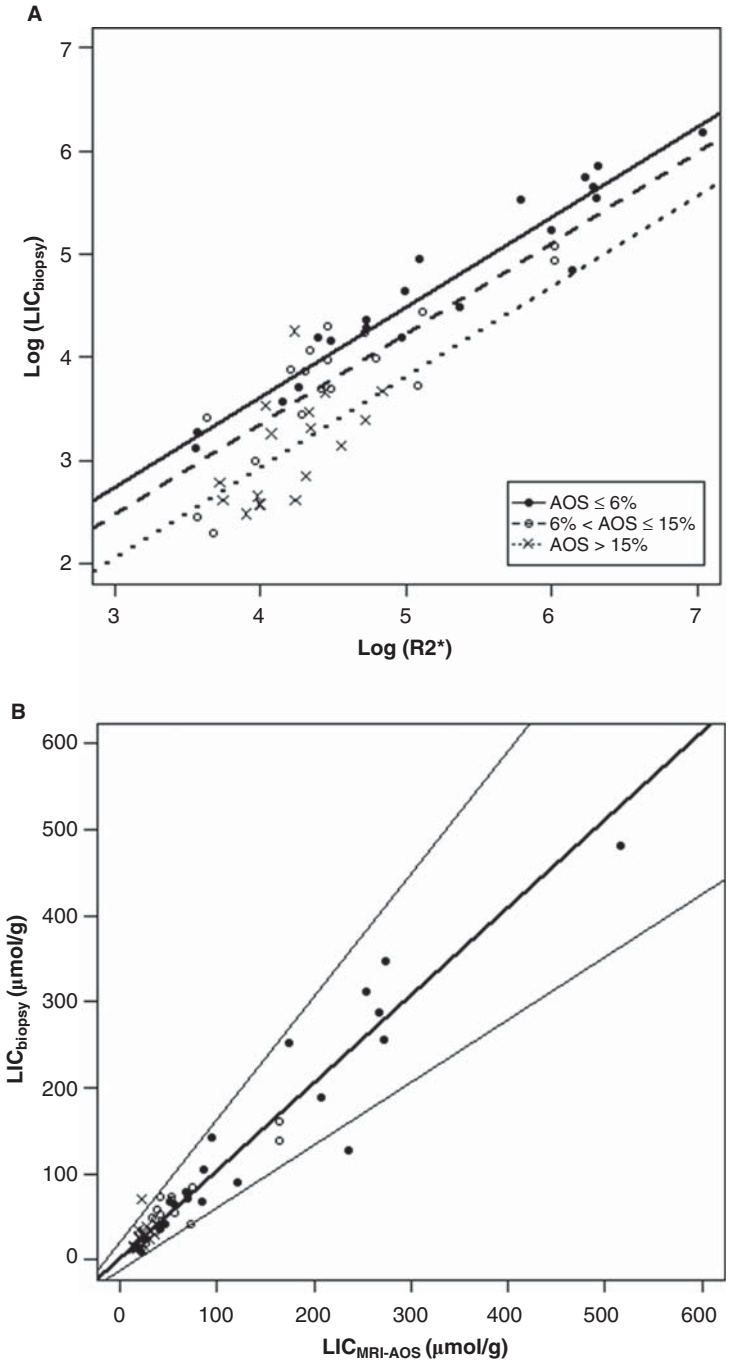

Figure 3. Quantification of hepatic iron by LIC through R2*, accounting for steatosis is shown. (A) R2*-LIC$_{biopsy}$ calibration lines on natural logarithmic scale, accounting for steatosis: AOS absent-to-mild (continuous), moderate (dashed), and severe (dotted) are shown. (B) Agreement between LIC$_{biopsy}$ and LIC$_{MRI-AOS}$ is shown. The solid line that represents the bias in using LIC$_{MRI-AOS}$ to predict LIC$_{biopsy}$ is superimposed to the 45° line of perfect agreement, whereas the two thin lines represent the 95% limits of agreement.
Abbreviations: AOS = Area of steatosis; LIC = Liver iron concentration.

of AOS$_{biopsy}$ in patients with moderate and severe iron overload were 3.2% and 0.5%, respectively.

The median of the 56 available MRI FF values was 16.0% (I–III quartiles = 9.7–21.8%), with a range between 1.6% and 33.1%. A threshold of 10.23% in FF differentiates patients with no-mild steatosis (AOS ≤6%) from those with moderate-to-severe AOS, with diagnostics performances of 97.5%

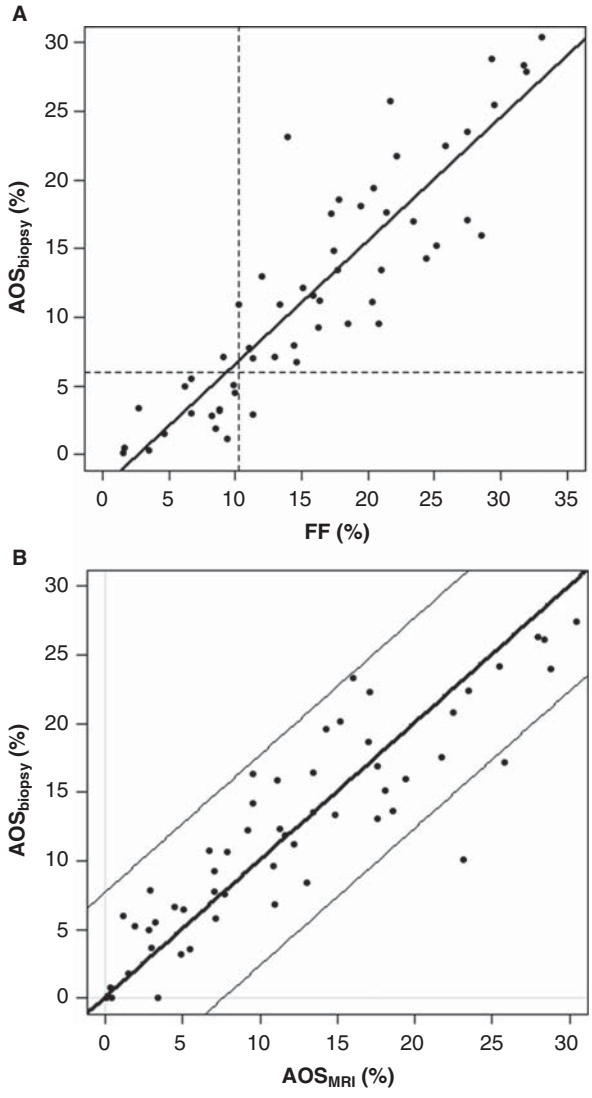

Figure 4. Quantification of hepatic fat as measured by AOS through FF is shown. (A) FF-AOS$_{biopsy}$ calibration line is shown. Dashed lines represent the cut-off for severity of steatosis. (B) Agreement between AOS$_{biopsy}$ and AOS$_{MRI}$ is shown. The solid line that represents the bias in using AOS$_{MRI}$ to predict AOS$_{biopsy}$ is superimposed on the 45° line of perfect agreement, whereas the two thin lines represent the 95% limits of agreement. Abbreviations: AOS = Area of steatosis; FF = Fat fraction; LIC = Liver iron concentration.

(95% CI = 87.1–99.6) and 93.8% (95% CI = 71.7–98.9) for sensitivity and specificity, respectively.

The relationship between AOS$_{biopsy}$ and FF is shown in Figure 4A, along with the calibration line needed to approximate liver steatosis by MRI: AOS$_{MRI}$ = −2.40 + 0.90FF (R^2 = 0.79). The results of the Bland and Altman analysis comparing AOS$_{biopsy}$ and AOS$_{MRI}$ showed a high global agreement, with a bias of −0.04% and limits of agreement equal to −7.7% and 7.7% (Figure 4B). The mean difference between AOS$_{biopsy}$ and AOS$_{MRI}$ was uniform over the range of measures (p = 0.151) with a constant variation in that range (p = 0.353). No further improvement in MRI measures of AOS was reached including either liver iron or other covariates in the calibration model.

Classification of patients into the four categories by AOS$_{MRI}$ and AOS$_{biopsy}$ is reported in Table IIc. AOS$_{MRI}$ accurately classified 47 out of 56 (84%) patients, with a weighted κ index of 0.84 (95% CI = 0.75–0.94%). All misclassifications occurred between contiguous classes, mainly between moderate and severe categories and vice-versa.

Internal validation

Data of the 10 patients used for blindly validating the results observed in the training sample are listed in Table III. The median AOS$_{biopsy}$ was 4.6% (range = 0.11–34.5%) and that of LIC$_{biopsy}$ was 51.9 μmol/g (range = 15.9–256.4 μmol/g).

Quantification of liver iron. The R2* cut-off of 147.07 s^{-1} resulted in two false-positives with LIC$_{biopsy}$ values just below the boundary of 100 μmol/g. When the more refined four categories stratification was used, two patients were misclassified: one had borderline levels between normal and mild iron overload (LIC$_{biopsy}$ = 27.4 μmol/g and LIC$_{MRI}$ = 30.9 μmol/g), whereas the other showed mild iron overload by LIC$_{biopsy}$ (93.3 μmol/g), but severe LIC$_{MRI}$ (295.5 μmol/g). The latter was regarded as an error of biochemical assessment of LIC, as the patient still had iron overload (serum ferritin = 1022 μg/L) after removing 8 g of iron by phlebotomies. The median of the errors made by replacing LIC$_{biopsy}$ with LIC$_{MRI}$ was 6.44 μmol/g and, as expected, the magnitude of the error increased with the increasing iron levels. No improvement was observed by correcting for steatosis.

Quantification of liver steatosis. The FF threshold of 10.2% fully discriminated between absent-to-mild and moderate-to-severe steatosis. In three patients, MRI parameter could not be calculated because of too much iron. Based on the results observed in the training sample, we assumed steatosis to be absent and this was indeed confirmed at liver biopsy (AOS$_{biopsy}$ <2%). In the remaining seven patients, we observed a single error in steatosis classification, regarding a subject with AOS$_{biopsy}$ of 13.9% (borderline between moderate and severe) whose steatosis was defined as severe based on MRI. The overall median difference between AOS$_{biopsy}$ and AOS$_{MRI}$ values was −0.22%. The largest error

Table III. Hepatic iron and fat values obtained by biopsy and predicted by MRI in the validation sample. Classes of severity of steatosis and iron overload are also reported.

ID	FF (%)	AOS_{biopsy} (%)		AOS_{MRI} (%)		R2* (sec^{-1})	LIC_{biopsy} (μmol/g)		LIC_{MRI} (μmol/g)		$LIC_{MRI\text{-}AOS}$ (μmol/g)	
7	-	0.11	A	<2	A	369.46	118.0	Mo	175.81	Mo	193.15	Mo
3	3.53	0.18	A	0.78	A	161.39	87.6	M	74.91	M	93.97	M
6	-	1.20	A	<2	A	611.59	93.3	M	295.46	S	299.46	S
5	-	1.73	A	<2	A	761.32	256.4	S	370.22	S	362.31	S
8	6.32	3.06	M	3.28	M	68.25	27.4	A	30.87	M	44.44	M
1	11.07	6.22	Mo	7.56	Mo	143.36	66.9	M	66.31	M	65.36	M
10	20.98	13.93	Mo	16.48	S	101.17	36.9	M	46.31	M	31.71	M
9	25.26	21.34	S	20.33	S	65.74	15.9	A	29.70	A	21.79	A
2	21.90	22.49	S	17.31	S	48.36	22.2	A	21.65	A	16.69	A
4	24.36	34.53	S	19.52	S	65.62	27.8	A	29.65	A	21.76	A

Abbreviations: A = Absent; AOS = Area of steatosis; FF = Fat fraction; LIC = Liver iron concentration; M = Mild; Mo = Moderate; S = Severe.

(15.0%) was found in a patient with AOS_{biopsy} of 34.5%, which was outside the range evaluated in the training sample (30.4%).

Discussion

In the present study, we demonstrated that single breath-hold multiecho MRI (at 1.5T) is a valid method to measure both liver iron content and the severity of steatosis in patients presenting with hyperferritinemia. This is an important issue in the clinical practice because: i) increased serum ferritin is frequently observed in patients with chronic liver diseases of any cause, but it is often an unreliable index of iron overload due to hepatocellular necrosis and cytokine activation; ii) iron overload can occur concomitantly with NAFLD; and iii) iron and fat can influence the prognosis of several hepatic disorders [1,2,4,10].

By the proposed calibration equations based on MRI parameters, we were able to simultaneously and accurately quantify iron and fat, and were able to obtain a more refined classification into four categories (absent, mild, moderate, and severe). Errors in LIC_{MRI} estimation increased with increasing iron accumulation as previously reported [29–32], whereas errors in AOS_{MRI} did not depend on the degree of steatosis. Studies suggested that there is an intrinsic heterogeneity of iron deposition within the liver that may explain much of the disagreement between MRI and biopsy [29,31], and that from a pragmatic standpoint, provided that MRI is accurate, management decisions do not rely in general on perfect determination of liver iron, but rather on the correct stratification in classes of iron overload severity.

In the present study, patients' classification predicted by MRI reflected the measures obtained by liver biopsy for both iron and fat, with only minor discrepancies. Most of the misclassifications for LIC concerned patients with absent-to-mild iron overload that would not be required to be iron depleted, whereas in two cases they concerned misclassification in the moderate-marked range of iron overload that would have required therapeutic intervention, anyway. Likewise, the internal validation showed good performances. The predictions of hepatic iron were reliable within the observed LIC range of 9.9–481.6 μmol/g. This range covers the amount of hepatic iron accumulation commonly seen in patients with hemochromatosis, DIOS, and with other chronic liver diseases, and expands the limit of consistency of Gandon et al.'s method (60–375 μmol/g) [32]. The reliability of predictions for steatosis spanned over a large range of fat accumulation (AOS: 0.10–30.42%; percentage of fatty hepatocytes: 2–98%) (Supplementary Figure 1). When MRI parameters for fat were not measurable in patients with high amount of hepatic iron, we assumed that these patients had very low-to-absent steatosis based on the findings observed in the training set and this assumption was indeed confirmed by liver histology. Thus, MRI information was almost completely in line with that obtained from liver biopsy.

This is, in our knowledge, the largest series reporting simultaneous evaluation of liver fat and iron by MRI compared to histological gold standards. There is much published research on liver T2*-R2* methods in samples of maximum 43 patients, mainly with sickle-cell anemia and thalassemia [31,33,34]. Our proposal, based on a log-linear calibration, is in complete agreement with Hankins et al.'s [34], and partially with Wood et al.'s [31], for LIC values ≤300 μmol/g (i.e. R2* ≤600 sec^{-1}) (Supplementary Figure 2). Similarly, MRI was also demonstrated to be an accurate technique in quantifying hepatic steatosis [13,19,35–37]. To the best of our knowledge, only one recent study analyzed both fat and iron in

31 patients [38]. At variance with our study, they measured hepatic FF and iron content using two different sequences, and classified steatosis based on the percentage of fatty hepatocytes, reporting lower performances (83% of sensitivity and 88% specificity) compared to our results (97.5% and 93.8%, respectively). Two studies used morphometric image analysis of hepatic steatosis to assess the diagnostic efficacy of MRI in patients with NAFLD or AFLD [35,39] and found a positive linear relationship between MRI (FF) and histology. However, in both studies no simultaneous measurement of liver iron was reported.

Although our study showed good performances for liver iron and fat estimates in both the training and validation samples, it would be desirable to assess whether our findings can be generalized to other MRI facilities and patients.

Conclusion

In conclusion, our results indicate that single breath-hold multiecho MRI (at 1.5T) is highly accurate for noninvasive estimates of hepatic iron and fat over a large relevant range. Our results may have a relevant impact in the diagnostic and therapeutic setting of patients with hyperferritinemia allowing to: i) rapidly define the meaning of hyperferritinemia (too much iron or too much fat), reducing the number of visits to healthcare facilities and repeated laboratory tests; ii) identify who benefits of iron depletion therapy and who does not, reducing the risk of iron deficiency or anemia induced by inappropriate phlebotomies; iii) define who benefits of dietary or other treatments (for liver fat) and monitoring its efficacy; iv) address the genetic diagnostic workout (e.g. molecular testing for diagnosis of rare forms of hemochromatosis); and v) limit the use of liver biopsy only when histology is important for patient management (fibrosis assessment). So, liver biopsy for the sole purpose of iron or fat determination would not be needed when MRI is available.

Acknowledgment

The research was partially supported by the "Associazione per lo Studio dell'Emocromatosi e delle Malattie da Sovraccarico di Ferro-ONLUS", Monza, Italy.

Declaration of interest: The authors report no conflicts of interest. The authors alone are responsible for the content and writing of the paper.

References

[1] Aguilar-Martinez P, Schved JF, Brissot P. The evaluation of hyperferritinemia: an updated strategy based on advances in detecting genetic abnormalities. Am J Gastroenterol 2005; 100:1185–94.

[2] Alla V, Bonkovsky HL. Iron in nonhemochromatotic liver disorders. Semin Liver Dis 2005;25:461–72.

[3] Trombini P, Piperno A. Ferritin, metabolic syndrome and NAFLD: elective attractions and dangerous liaisons. J Hepatol 2007;46:549–52.

[4] Dongiovanni P, Fracanzani AL, Fargion S, Valenti L. Iron in fatty liver and in the metabolic syndrome: a promising therapeutic target. J Hepatol 2011;55:920–32.

[5] Mendler MH, Turlin B, Moirand R, Jouanolle AM, Sapey T, Guyader D, et al. Insulin resistance-associated hepatic iron overload. Gastroenterology 1999;117:1155–63.

[6] Riva A, Trombini P, Mariani R, Salvioni A, Coletti S, Bonfadini S, et al. Revaluation of clinical and histological criteria for diagnosis of dysmetabolic iron overload syndrome. World J Gastroenterol 2008;14:4745–52.

[7] Bozzini C, Galbiati S, Tinazzi E, Aldigeri R, De Matteis G, Girelli D. Prevalence of hereditary hyperferritinemia-cataract syndrome in blood donors and patients with cataract. Haematologica 2003;88:219–20.

[8] Piperno A, Trombini P, Gelosa M, Mauri V, Pecci V, Vergani A, et al. Increased serum ferritin is common in men with essential hypertension. J Hypertens 2002;20:1513–18.

[9] Martinelli N, Traglia M, Campostrini N, Biino G, Corbella M, Sala C, et al. Increased serum hepcidin levels in subjects with the metabolic syndrome: a population study. PLoS One 2012;7:e48250.

[10] Adams PC, Barton JC. A diagnostic approach to hyperferritinemia with a non-elevated transferrin saturation. J Hepatol 2011;55:453–8.

[11] Starley BQ, Calcagno CJ, Harrison SA. Nonalcoholic fatty liver disease and hepatocellular carcinoma: a weighty connection. Hepatology 2010;51:1820–32.

[12] Bassett ML, Hickman PE, Dahlstrom JE. The changing role of liver biopsy in diagnosis and management of haemochromatosis. Pathology 2011;43:433–9.

[13] Springer F, Machann J, Claussen CD, Schick F, Schwenzer NF. Liver fat content determined by magnetic resonance imaging and spectroscopy. World J Gastroenterol 2010;16:1560–6.

[14] Franzen LE, Ekstedt M, Kechagias S, Bodin L. Semiquantitative evaluation overestimates the degree of steatosis in liver biopsies: a comparison to stereological point counting. Mod Pathol 2005;18:912–16.

[15] Cesbron-Metivier E, Roullier V, Boursier J, Cavaro-Ménard C, Lebigot J, Michalak S, et al. Noninvasive liver steatosis quantification using MRI techniques combined with blood markers. Eur J Gastroenterol Hepatol 2010;22: 973–82.

[16] Turlin B, Ramm GA, Purdie DM, Lainé F, Perrin M, Deugnier Y, et al. Assessment of hepatic steatosis: comparison of quantitative and semiquantitative methods in 108 liver biopsies. Liver Int 2009;29:530–5.

[17] Tziomalos K, Perifanis V. Liver iron content determination by magnetic resonance imaging. World J Gastroenterol 2010; 16:1587–97.

[18] Wood JC. Magnetic resonance imaging measurement of iron overload. Curr Opin Hematol 2007;14:183–90.

[19] Lee SS, Park SH, Kim HJ, Kim SY, Kim MY, Kim DY, et al. Non-invasive assessment of hepatic steatosis: prospective

comparison of the accuracy of imaging examinations. J Hepatol 2010;52:579–85.
[20] Bydder M, Shiehmorteza M, Yokoo T, Sugay S, Middleton MS, Girard O, et al. Assessment of liver fat quantification in the presence of iron. Magn Reson Imaging 2010;28:767–76.
[21] Westphalen AC, Qayyum A, Yeh BM, Merriman RB, Lee JA, Lamba A, et al. Liver fat: effect of hepatic iron deposition on evaluation with opposed-phase MR imaging. Radiology 2007;242:450–5.
[22] O'Regan DP, Callaghan MF, Wylezinska-Arridge M, Fitzpatrick J, Naoumova RP, Hajnal JV, et al. Liver fat content and T2*: simultaneous measurement by using breath-hold multiecho MR imaging at 3.0 T–feasibility. Radiology 2008;247:550–7.
[23] Ishak K, Baptista A, Bianchi L, Callea F, De Groote J, et al. Histological grading and staging of chronic hepatitis. J Hepatol 1995;22:696–9.
[24] Barry M, Sherlock S. Measurement of liver-iron concentration in needle-biopsy specimens. Lancet 1971;1:100–3.
[25] Adams P, Brissot P, Powell LW. EASL international consensus conference on haemochromatosis. J Hepatol 2000;33:485–504.
[26] Deugnier YM, Loreal O, Turlin B, Guyader D, Jouanolle H, Moirand R, et al. Liver pathology in genetic hemochromatosis: a review of 135 homozygous cases and their bioclinical correlations. Gastroenterology 1992;102:2050–9.
[27] Kleiner DE, Brunt EM, Van Natta M, Behling C, Contos MJ, Cummings OW, et al. Design and validation of a histological scoring system for nonalcoholic fatty liver disease. Hepatology 2005;41:1313–21.
[28] Carstensen B. Statistics in practice, in comparing clinical measurement methods: a practical guide. John Wiley & Sons, Ltd, Chichester, UK; 2010, doi: 10.1002/9780470683019.scard.
[29] St Pierre TG, Clark PR, Chua-anusorn W, Fleming AJ, Jeffrey GP, Olynyk JK, et al. Noninvasive measurement and imaging of liver iron concentrations using proton magnetic resonance. Blood 2005;105:855–61.
[30] Bonkovsky HL, Rubin RB, Cable EE, Davidoff A, Rijcken TH, Stark DD. Hepatic iron concentration: noninvasive estimation by means of MR imaging techniques. Radiology 1999;212:227–34.
[31] Wood JC, Enriquez C, Ghugre N, Tyzka JM, Carson S, Nelson MD, et al. MRI R2 and R2* mapping accurately estimates hepatic iron concentration in transfusion-dependent thalassemia and sickle cell disease patients. Blood 2005;106:1460–5.
[32] Gandon Y, Olivie D, Guyader D, Aubé C, Oberti F, Sebille V, et al. Non-invasive assessment of hepatic iron stores by MRI. Lancet 2004;363:357–62.
[33] Anderson LJ, Holden S, Davis B, Prescott E, Charrier CC, Bunce NH, et al. Cardiovascular T2-star (T2*) magnetic resonance for the early diagnosis of myocardial iron overload. Eur Heart J 2001;22:2171–9.
[34] Hankins JS, McCarville MB, Loeffler RB, Smeltzer MP, Onciu M, Hoffer FA, et al. R2* magnetic resonance imaging of the liver in patients with iron overload. Blood 2009;113:4853–5.
[35] House MJ, Gan EK, Adams LA, Ayonrinde OT, Bangma SJ, Bhathal PS, et al. Diagnostic performance of a rapid magnetic resonance imaging method of measuring hepatic steatosis. PLoS One 2013;8:e59287.
[36] Noureddin M, Lam J, Peterson MR, Middleton M, Hamilton G, Le TA, et al. Longitudinal comparison between MRI, MRS and histology-determined steatosis in. NAFLD patients at two-time points in a randomized trial. Hepatology 2013;58:1930–40.
[37] Permutt Z, Le TA, Peterson MR, Seki E, Brenner DA, Sirlin C, et al. Correlation between liver histology and novel magnetic resonance imaging in adult patients with non-alcoholic fatty liver disease - MRI accurately quantifies hepatic steatosis in NAFLD. Aliment Pharmacol Ther 2012;36:22–9.
[38] Benjamin H, Christian K, Stefan R, Eder R, Judmaier W, Zoller H, et al. Evaluation of liver fat in the presence of iron with MRI using T2* correction: a clinical approach. Eur Radiol 2013;23:1643–9.
[39] D'Assignies G, Ruel M, Khiat A, Lepanto L, Chagnon M, Kauffmann C, et al. Noninvasive quantitation of human liver steatosis using magnetic resonance and bioassay methods. Eur Radiol 2009;19:2033–40.

Supplementary materials available online

Supplementary Materials and Methods and Supplementary Figure 1 and 2.